

## Forming method of wick structure for heat column

TAO Su-lian<sup>1,2</sup>, TANG Yong<sup>1</sup>, PAN Min-qiang<sup>1</sup>, WAN Zhen-ping<sup>1</sup>, LU Long-sheng<sup>1</sup>

1. Key Laboratory of Surface Functional Structure Manufacturing of Guangdong Higher Education Institutes, South China University of Technology, Guangzhou 510640, China;

2. Department of Mechanical Engineering, Guangdong Technical College of Water Resources and Electric Engineering, Guangzhou 510635, China

Received 1 November 2010; accepted 30 March 2011

**Abstract:** The intensified boiling and condensation wick structures of heat column were designed and manufactured by ploughing-extrusion (P-E) machining method. The forming process and mechanism were analyzed. The results show that the P-E depth plays a decisive role in forming of wick structure. The larger the P-E depth is, the better the surface characteristics are. Only when the groove spacing is in a certain range, superior surface structure can be formed in the wick. The better enhancement boiling structure forms at P-E depth of 0.3 mm, ringed groove spacing of 0.4 mm, and interior angle of radial groove of 3°; the better enhancement condensation structure forms at P-E depth of 0.3 mm, ringed groove spacing of 0.4 mm, and axial grooves spacing of  $\pi/3$  mm.

**Key words:** heat column; wick; ploughing-extrusion; heat transfer; micro-groove

### 1 Introduction

The heat dissipation problem of high heat flux density is one of the key factors influencing the performances of electronic components [1–2]. Recently, the heat generated per unit area of electronic component increases fanatically, and the available space for installing thermal control devices decreases dramatically. Nowadays, micro heat pipe is regarded as one of the effective components to solve the high heat flux problem of electronic devices. It is usually bended in order to meet the space requirement, which leads to the reduction of heat transfer performances [3]; moreover, the heat transfer capability of micro heat pipe is also limited by the area of the evaporator and condenser. Therefore, multiple heat pipes are generally used for heat dissipation. Cylindrical heat pipe recently begins to appear to meet the cooling and space requirements for high-performance electronic components. Cylindrical heat pipe is also called as heat column. Unlike to common micro heat pipe, heat column is short and thick. It has rapid heat transfer rate, great heat capacity and good adaptability. Its heat capacity greatly exceeds that

of normal heat pipe.

Wick structure plays an important role in the heat transfer performance of heat column [4], so how to design wick structure to obtain optimal heat transfer performance is crucial for studying heat column. The available research on heat pipe focused mainly on theoretical model, heat transfer mechanism, performance test and so on [5–6]. However, until now, there are few reports about the study on the manufacture of heat pipe. KANG et al [7] fabricated radial micro grooved heat pipe of 5 cm×5 cm by micromachining and eutectic bonding technology. GILLOT et al [8] developed a plate silicon micro heat pipe with rectangular grooves by etching technology. LEE et al [9] reported the design and manufacturing of an integrated heat pipe system. A layer of nitride film covered on V-shape groove was fabricated by wafer bonding and reverse etching technology. CHEN and HSIEH [10] manufactured heat pipe with microgrooves of 200–500  $\mu\text{m}$  by chemical etching and precision machining method. LI and XIAO [11] proposed high-speed spinning method and machined an axial micro-grooved copper heat pipe. Nowadays the wick on the inner wall of heat pipe was manufactured mainly by micro etching and micro-processing methods,

but all the methods are either costly or complex.

In the present work, a new style wick structure was put forward to solve the problem of present high machining cost and low heat dissipation power for wick, multi-dimensional and multi-scale heat function surface structure was applied to the wick of heat column to enhance capillary force, enhancing its heat transfer performance. The wick structure of heat column was fabricated by P-E method. Corresponding formation characteristic, machining condition and formation mechanism were discussed, and the influence of P-E parameters on the wick surface was investigated.

## 2 Wick principle and design of wick structure of heat column

### 2.1 Wick principle of heat column

Heat column is a cylindrical copper sealed vacuum chamber, and there exists capillary structure on its inner wall. Its work principle is shown in Fig. 1. The bottom of heat column is the evaporation face contacting the heat source, and the surrounding is the condensation face playing a condensation role. When the heat column works, input heat passes the evaporative section, vaporizing the coolant liquid. Then the vapor transfers to condenser section. In the condenser section, the vapor releases latent heat and gets liquefied. The condensed liquid returns from the condenser to the evaporator through capillary structure, thus heat column completes a work cycle, so repeatedly, thereby the heat diffuses quickly from a concentrated area to the condenser.

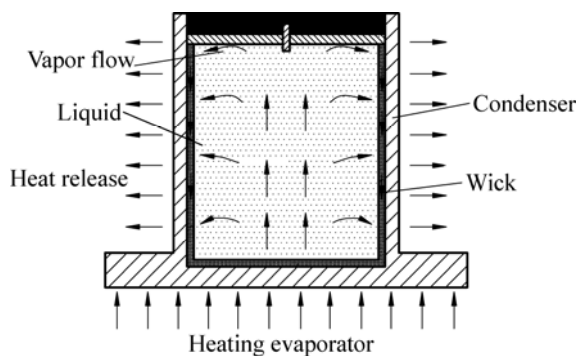


Fig. 1 Principle of heat column

### 2.2 Design of wick structure

The wick structure on the inner wall of heat column plays a crucial role in its heat transfer performance. The evaporator not only enhances boiling performance but also ensures condensed liquid return from the condenser to the evaporator. Rough surface can improve the boiling performance [12], thus increasing roughness of wick surface can enhance the capillary force of wick. Rough micro grooves were machined on the inner wall

of copper tube by P-E, and it can enhance the capillary force when being used in micro-grooved heat pipe [13–14]. The wick structure of heat column was fabricated by P-E method. The evaporator structure is shown in Fig. 2(a). The intersecting micro-grooves are machined by P-E. The groove surface is rough, and a large number of micro-holes come into being on the evaporator surface. Two-phase flow of steam and liquid can flow in staggered vertically and horizontally microgrooves to promote turbulence and boiling. The micro-groove structure is composed of micro-grooves, flanges and intermittent micro-fins. There are flanges between two micro-grooves, which have intermittent micro-fins promoting nucleate boiling. The main function of condenser is to ensure the vapor condensate and condensation liquid return from condenser to evaporator. Figure 2(b) shows the structure of condenser. Micro channel finned cooling structure surface utilizes cross groove fin structure, which is composed of micro-grooves, flanges and intermittent micro-fins. Two-phase flow of steam and liquid can flow in vertical and horizontal micro-channel, and the fins around microgrooves are propitious to nucleate boiling and convection.

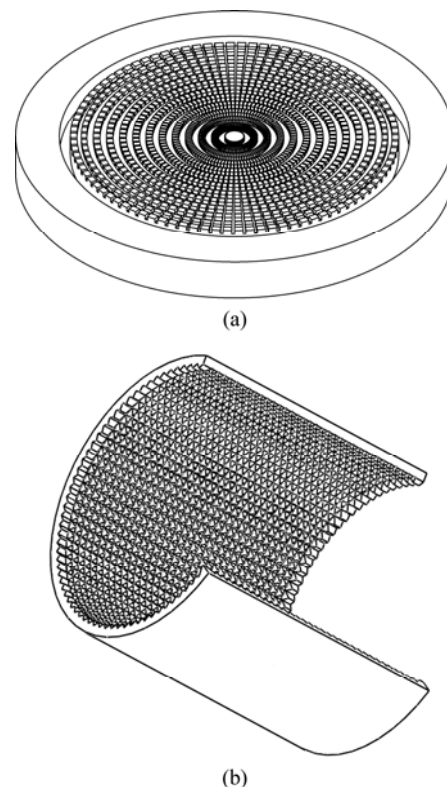


Fig. 2 Wick structure on evaporator (a) and condenser (b) of heat column

## 3 Experimental

The experiment was carried out on the lathe

C6132A1. A red copper rod with a diameter of 40 mm and a thickness of 2 mm was utilized to fabricate the evaporator. The material of condenser was red copper tube with a diameter of 32 mm and a thickness of 1 mm. The tool was made of high speed steel W18Cr4V. The wick of evaporator was machined twice. At first, the work piece was fixed in the lathe chuck, the main spindle rotated and drove copper rod to rotate, the P-E tool was fixed on knife nest, the P-E tool fed radially at the same time and then a series of ringed micro-grooves were formed on the surface of copper rod, as shown in Fig. 3. Next, the work piece was fixed, the P-E tool rotated 90°, the tool moved radially, and then a radial groove perpendicular to ringed grooves was formed; then the lathe chuck rotated a certain angle, the tool moved radially too, a second radial groove was formed, and so on. Thus, a series of radial grooves were formed and then three-dimensional fins were formed. The wick structure of condenser was formed twice too, a mould was fixed outside of copper tube in order to reduce the deformation of copper tube. The copper tube was fixed in the lathe chuck, the main spindle rotated to drive copper tube to rotate, the P-E tool was fixed on a home made knife nest which was fixed on the knife nest of lathe chuck, the tool fed axially at the same time, then a series of ringed micro-grooves were formed on the inner wall of copper tube. The processing diagram is shown in Fig. 4. The copper tube was fixed during the second forming, the P-E tool moved axially, thus an axial groove perpendicular to the ringed grooves was formed. Then, the lathe chuck rotated a certain angel, the second groove was formed too, and so on, a series of axial grooves were formed, thus multi-scale fin structure was formed.

The schematic diagram of the forming tool is shown in Fig. 5. It consists of a ploughing edge, a primary extruding face  $A_\gamma$ , a minor extruding face  $A_{\gamma'}$ , a primary forming face  $A_\beta$  and a minor forming face  $A_{\beta'}$ ;  $\gamma_0$  is the primary extruding angle;  $\gamma_0'$  is the minor extruding

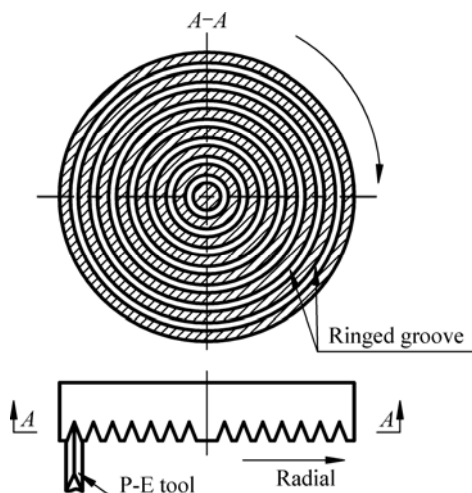


Fig. 3 Processing schematic diagram of evaporator

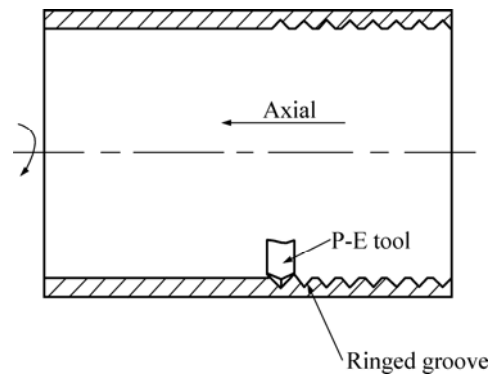


Fig. 4 Processing schematic diagram of condenser

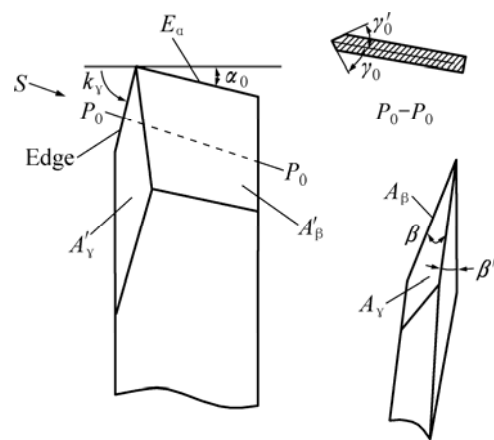


Fig. 5 Schematic diagram of P-E tool

angle;  $\beta$  is the primary forming angle;  $\beta'$  is the minor forming angle ( $k_\gamma$  is the inclination angle;  $\alpha_0$  is the angle of backing off;  $E_\alpha$  is the flank)[15].

## 4 Results and discussion

P-E is a micro-chip ploughing composite processing method, and the principle involves metal cutting and plastic deformation. P-E process can be divided into plow cutting stage, extrusion stage and fin formation stage. The work piece is fixed on a lathe rotates, and the tool moves linearly when it adjusts the extrusion depth. The tool contacts work piece surface, and gradually cuts into the metal matrix, metal is split, the tool squeezes the metal to form two dimensional fins, and then the micro-grooves perpendicular to the grooves formed at first time are machined on the base of the two-dimensional fins. At last, three dimensional fins are formed when the grooves formed at the second time influence that formed at first time.

### 4.1 Impact of processing parameters on wick structure of evaporator

#### 4.1.1 P-E depth $a_p$

The wick surface morphology of evaporator is

shown in Fig. 6 at same groove spacing  $f$  and different P-E depth  $a_p$ . The depth of P-E is a key factor affecting the surface characteristic of wick. Figure 6(a) shows the surface morphology under the condition that the ringed groove spacing  $f_r$  is 0.2 mm, the angle  $\theta$  between adjacent radial grooves is  $2^\circ$  and the radial and circular groove depth  $a_p$  values are both 0.1 mm, small V-type semi-enclosed shallow holes and a large number of microscopic holes are formed to cover the surface. With severe plastic deformation and extrusion effect of metal, micro holes are shaped like spacial curved surface, a large number of sharp corners and depressed tearing organizations are formed around the holes. When the P-E depth is increased to 0.2 mm, V-type holes gradually change into U-type holes, the formation of radial grooves makes great impact on ringed grooves, and obvious deformation occurs on the ringed grooves. The U-type holes are formed by ringed grooves and radial grooves. The area, volume and depth of U-type holes are larger than those of V-shape holes formed at the P-E depth of 0.1 mm. When the P-E depth increases to 0.3 mm, the

area, volume and depth of U-type holes continue increasing, meanwhile radial grooves play a right impact on ringed grooves, then U-type holes are formed on the surface of wick. It can be found from experiment that the greater the P-E depth, the larger the plastic deformation, the greater the influence of radial groove on ringed groove, the more favorable the formation of spacial fins. But the P-E depth is restricted by tool strength and system stiffness, too large P-E depth makes the tool deform and even collapse, and affects the formation of surface boiling structure.

#### 4.1.2 Ringed groove spacing

Figure 7 shows SEM images of evaporator surface structure at the P-E depth of 0.2 mm, the radial groove angle of  $4^\circ$  and different ringed groove spacing values. It can be seen from Fig. 7 that when  $f_r$  is 0.2 mm, the plastic deformation occurring on axial grooves impacts ringed grooves greatly, which results in sharp bent deformation occurring to ringed grooves. When the ringed grooves are forming, all the grooves are squeezed, and the crowded narrow U-type spacial grooves are

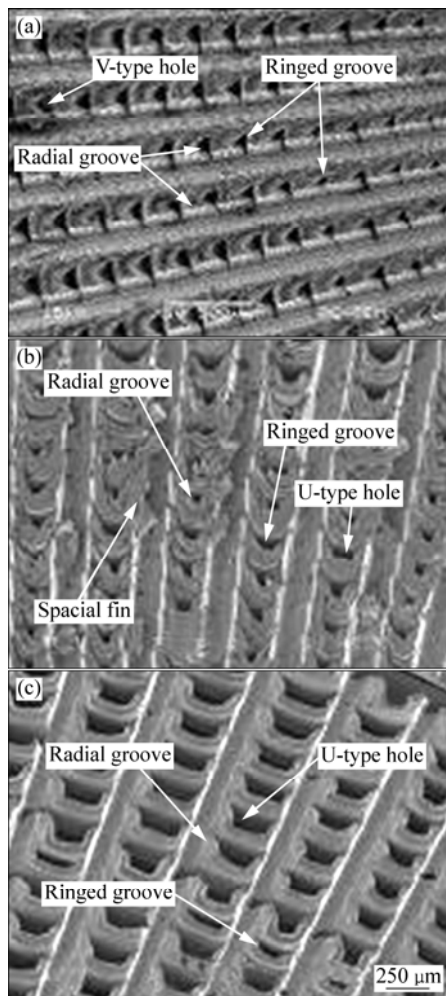


**Fig. 6** Groove topographs of wick at different P-E depth: (a)  $a_p=0.1$  mm,  $f_r=0.2$  mm,  $\theta=2^\circ$ ; (b)  $a_p=0.2$  mm,  $f_r=0.2$  mm,  $\theta=2^\circ$ ; (c)  $a_p=0.3$  mm,  $f_r=0.2$  mm,  $\theta=2^\circ$

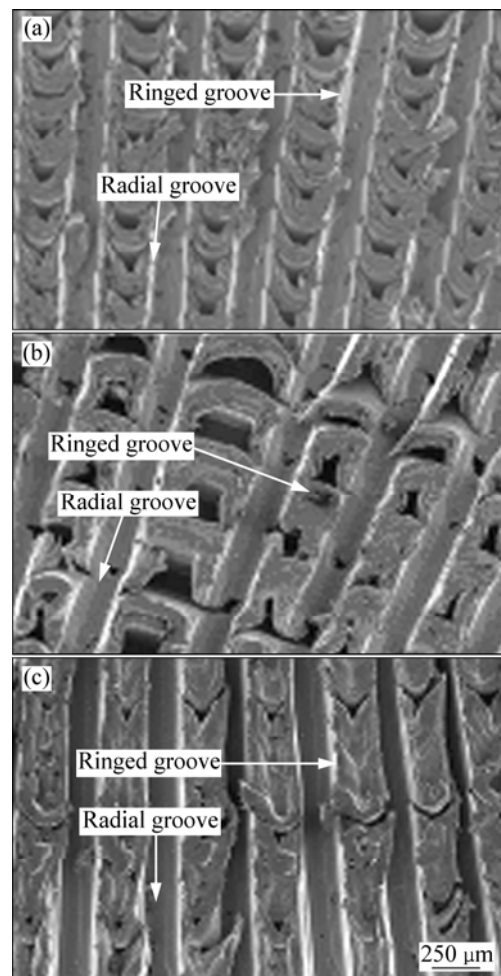


**Fig. 7** Groove topographs of wick at different ringed groove spacing values: (a)  $a_p=0.2$  mm,  $f_r=0.2$  mm,  $\theta=2^\circ$ ; (b)  $a_p=0.2$  mm,  $f_r=0.4$  mm,  $\theta=2^\circ$ ; (c)  $a_p=0.2$  mm,  $f_r=0.6$  mm,  $\theta=2^\circ$

formed on the wick surface, the formed spacial fins by P-E are around the grooves, and many burrs are formed around spacial fins under P-E action. With increasing ringed groove spacing, the impact of the formation of one ringed groove on the adjacent ringed groove is less and less. When  $f_r$  is 0.4 mm, the bent deformation lessens a little, the impact made by the formation of radial grooves on the ringed grooves weakens, the area and volume of U-type holes increase, and the burrs around holes decrease. When  $f_r$  is 0.6 mm, the bent deformation between the adjacent ringed grooves is very little. The formation of radial grooves has little impact on the ringed groove, the depth of U-type holes lowers, and no burrs are formed around the holes.

#### 4.1.3 Radial groove angle $\theta$

Figure 8 shows the wick surface morphology at P-E depth of 0.2 mm, and different radial groove spacing values. When  $\theta$  is  $2^\circ$  (see Fig. 8(a)), the forming of radial grooves has great impact on ringed grooves, severe plastic bent deformation occurs on the ringed grooves, and narrow U-type holes are formed on the surface of metal. The fins around U-type holes are

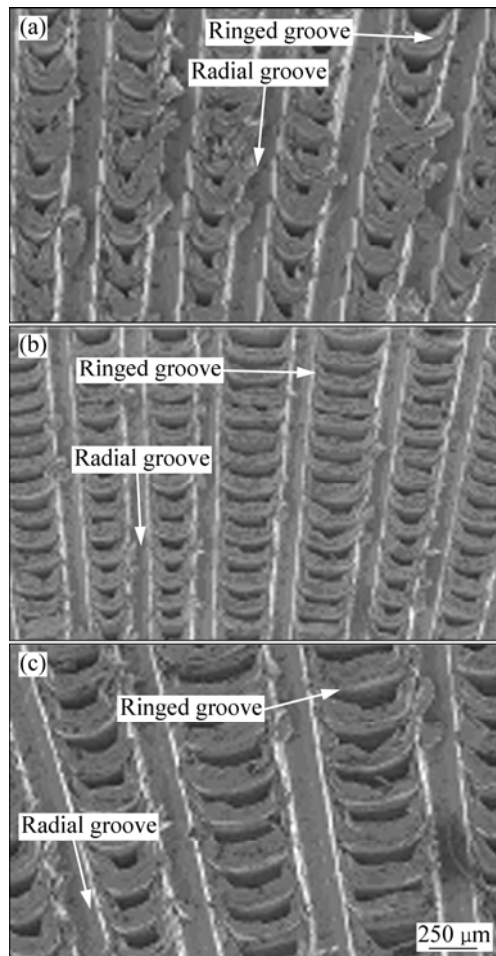


**Fig. 8** Groove topographs of wick at different radial groove angle: (a)  $a_p=0.2$  mm,  $f_r=0.2$  mm,  $\theta=2^\circ$ ; (b)  $a_p=0.2$  mm,  $f_r=0.2$  mm,  $\theta=3^\circ$ ; (c)  $a_p=0.2$  mm,  $f_r=0.2$  mm,  $\theta=4^\circ$

squeezed to arch, then many burrs are formed around holes. When  $\theta$  is  $3^\circ$  (see Fig. 8(b)), the impact made by the forming of radial grooves on ringed groove weakens, the bent deformation of ringed grooves decreases, the volume and area of holes increase, further the burrs of fins around U-type holes decrease greatly. The larger the  $\theta$  is, the less the impact made by the forming of radial grooves on ringed grooves is, the wider the U-type grooves formed by adjacent two circular grooves and radial grooves are, the shallower the spacial fins are.

The results show that the P-E depth, ringed groove spacing and radial groove angle determine the groove wick surface morphology together. The greater the P-E depth is, the deeper the formed holes are, the better the surface morphology of spacial fins are; the wider the ringed groove spacing is, the less the impact made by one ringed groove on the adjacent ringed groove is, the less the bent deformation occurring to ringed groove is. When the ringed groove spacing is too wide, there is no mutual impact between two adjacent ringed grooves, which is not conducive to the formation of spacial fins. The greater the radial groove angle, the less the impact made by the formation of radial groove on ringed groove. On the contrary, if the impact is too large, it is unfavorable to the formation of wick boiling surface structure. The experimental evaporator wick achieves better enhancement boiling structure when the P-E depth  $a_p$  is 0.3 mm, the circular groove spacing  $f_r$  is 0.4 mm, and the radial groove angle  $\theta$  is  $3^\circ$ .

## 4.2 Influence of processing parameters on wick of condenser

### 4.2.1 P-E depth $a_p$

Figure 9 shows the surface morphology of condenser at axial groove spacing  $f_\theta$  of  $\pi/3$  mm, ringed groove spacing of 0.4 mm and different P-E depth values. When  $a_p$  is 0.1 mm, a little bent deformation occurs to the ringed grooves, there is almost no impact between two adjacent ringed grooves, the impact made by the forming of axial grooves on ringed groove is little, then little and shallow grooves are formed on the surface of wick, and shallow fins are formed around grooves. When  $a_p$  is 0.2 mm, the depth of formed holes and the height of fins increase, and many burrs appear around fins. When  $a_p$  is 0.3 mm, the forming of one ringed groove impacts adjacent ringed grooves greatly, severe plastic bent deformation occurs on ringed grooves, the formation of axial groove impacts ringed groove greatly, deeper spacial holes are formed on the wick surface, and the parabolic curved surface fins are formed around holes. Under the same condition, the larger the P-E depth is, the bigger and deeper spacial grooves are, the higher the spacial fins are. However, the tool is constrained by tool

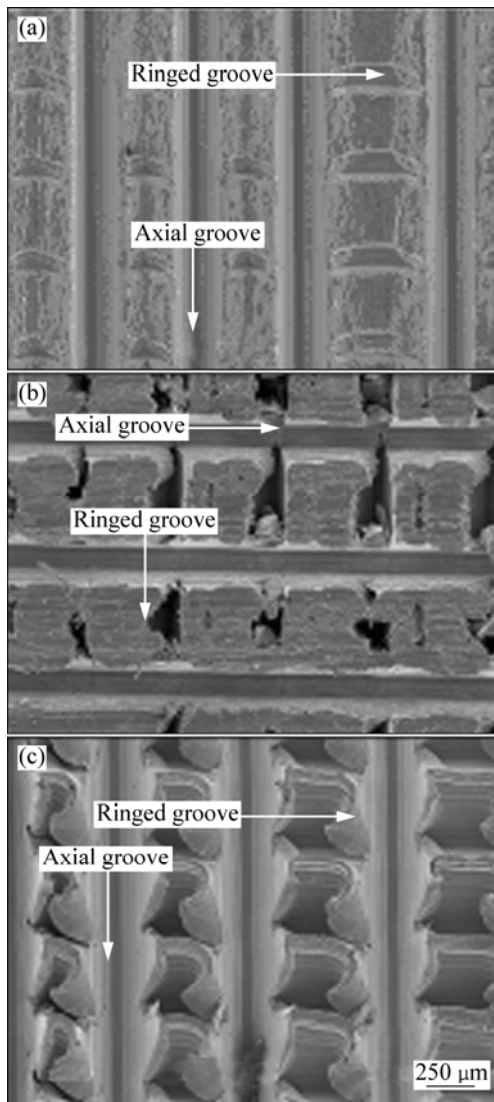


**Fig. 9** Groove topographs of wick for condenser at different P-E depth values: (a)  $a_p=0.1$  mm,  $f_r=0.4$  mm,  $f_\theta=\pi/3$  mm; (b)  $a_p=0.2$  mm,  $f_r=0.4$  mm,  $f_\theta=\pi/3$  mm; (c)  $a_p=0.3$  mm,  $f_r=0.4$  mm,  $f_\theta=\pi/3$  mm

strength and system stiffness, P-E depth can not be too large.

#### 4.2.2 Ringed groove space $f_r$

Figure 10 shows the surface structure on the inner wall of copper tube at the P-E depth of 0.3 mm, the axial groove spacing of  $\pi/3$  mm and different ringed groove spacings. When  $f_r$  is 0.2 mm, great impact occurs between two adjacent ringed grooves, the spacial grooves can not be formed on the inner surface of copper tube, and the formed spacial fins are not obvious; when the ringed groove spacing is 0.6 mm, obvious spacial grooves come into being, the grooves are mouth-type grooves depressed at center and arched around, the depth and surface area of holes are not large and the fins are not high. When the ringed groove spacing is 0.4 mm, one groove impacts another groove and the axial grooves

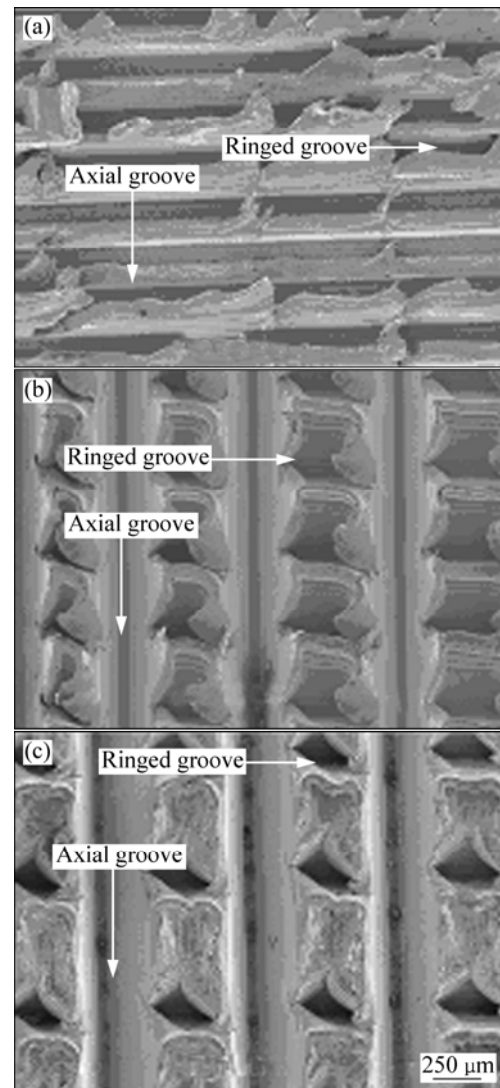


**Fig. 10** Groove topographs of wick for condenser at different ringed spacings: (a)  $a_p=0.3$  mm,  $f_r=0.2$  mm,  $f_\theta=\pi/3$  mm; (b)  $a_p=0.3$  mm,  $f_r=0.4$  mm,  $f_\theta=\pi/3$  mm; (c)  $a_p=0.3$  mm,  $f_r=0.6$  mm,  $f_\theta=\pi/3$  mm

have great influence on ringed grooves, parabolic type spacial grooves depressed in the center and arched around are formed on the inner wall of copper tube, obvious spacial fins are formed around holes. When the ringed groove spacing is too narrow, much interference occurs between adjacent annular grooves, which are not conducive to the formation of fins. But when the ringed groove spacing is too wide, little interference occurs between adjacent ringed grooves, the fins formed on the inner wall of copper tube are not obvious. Only when the orbicular groove spacing is within a certain range, it is right for the interference between two adjacent grooves, and the fins formed are very obvious.

#### 4.2.3 Axial groove spacing $f_\theta$

Figure 11 shows the surface morphology of the inner wall of copper pipe at the P-E depth of 0.3 mm, the

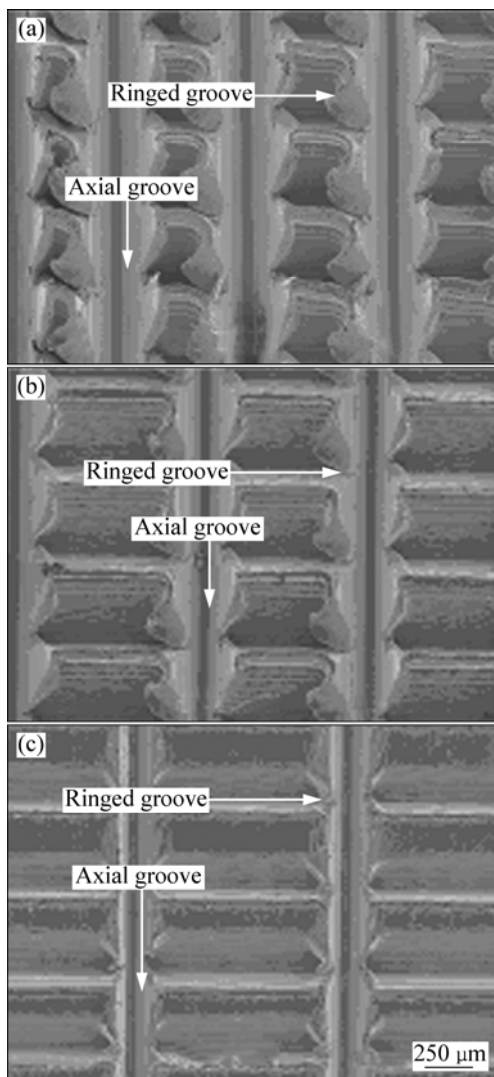


**Fig. 11** Groove topographs of wick for condenser at different axial groove spacings: (a)  $a_p=0.1$  mm,  $f_r=0.4$  mm,  $f_\theta=\pi/3$  mm; (b)  $a_p=0.2$  mm,  $f_r=0.4$  mm,  $f_\theta=\pi/2$  mm; (c)  $a_p=0.3$  mm,  $f_r=0.4$  mm,  $f_\theta=2/3\pi$  mm

ringed groove spacing of 0.4 mm and different  $f_\theta$  values. When  $f_\theta$  is  $\pi/3$  mm, the good condensation structure is formed on the inner surface of copper tube. With increasing  $f_\theta$ , the formation of axial grooves has less impact on ringed grooves, the shallower spacial grooves are formed on the inner surface of copper tube, and the formed spacial fins are not obvious. When  $f_\theta$  is larger than a critical value, the influence between adjacent grooves is less and less, the formed surface fins are not more and more obvious. Otherwise, when  $f_\theta$  is less than a critical value, a great mutual impact occurs between adjacent ringed grooves, it is not conducive to the forming of spacial fins. P-E depth, ringed groove spacing and axial groove spacing determine the condensation wick structure together. P-E depth plays a decisive role in wick surface morphology. The larger the P-E depth, the better the wick surface morphology; but the P-E

depth is restricted by the tool strength and system rigidity, the maximum P-E depth is 0.3 mm. The ringed groove and axial groove spacings both have a certain critical value, it is not conducive to the forming of the spacial grooves and fins when the groove spacing is not equal to the critical value. Experimental results show that the experimental condenser wick obtains better condensation structure when  $a_p$  is 0.3 mm,  $f_r$  is 0.4 mm and  $f_\theta$  is  $\pi/3$  mm.

## 5 Conclusions

1) The wick structures on evaporator and condenser of heat column are designed, and the coarse surface structure of wick is formed by P-E method. The designed evaporation structure is conducive to evaporator boiling; the designed condensation structure favors the return of the condensating liquid.

2) P-E depth plays a decisive role in the wick surface morphology. The larger the P-E depth, the better the surface morphology. But it is limited by tool strength and system stiffness, the P-E depth can not be too large; when the circular groove spacings  $f_\theta$  and  $f_r$  are only in a certain range, better surface topography can be formed; on the contrary, it is not favorable to the forming of surface morphology.

3) The  $a_p$ ,  $f_r$  and  $f_\theta$  decide the surface topography of wick. The evaporation obtains better enhancement boiling structure at the P-E depth of 0.3 mm, the ringed groove spacing of 0.4 mm, the radial groove angle of  $3^\circ$ . The condenser wick achieves optimal condensation structure at the P-E depth of 0.3 mm, the ringed groove spacing of 0.4 mm, the radial groove spacing of  $\pi/3$  mm.

## References

- [1] RIGHTLEY M J, TIGGES C P, GIVLER R C, ROBINO C V, MULHALL J J, SMITH P M. Innovative wick design for multi-source flat plate heat pipes [J]. *Microelectronics Journal*, 2003, 34: 187–194.
- [2] JONES W K, LIU Y Q, GAO M C. Micro heat pipes in low temperature cofire ceramic (LTCC) substrates [J]. *IEEE Transactions on Components and Packaging Technologies*, 2003, 26(1): 110–115.
- [3] TAO Han-zhong, ZHAN Hong, ZHUANG Jun. Comparison of the heat transfer performance in an AGHP with and without  $90^\circ$  bend [J]. *Journal of Astronautic*, 2008, 29(2): 722–728.
- [4] WILLIAMS R R, HARRIS D K. A device and technique to measure the heat transfer limit of planar heat pipe wick [J]. *Experimental Thermal and Fluid Science*, 2006, 30: 277–284.
- [5] KIM S J, SEO J K, DO K H. Analytical and experimental investigation on the operational characteristics and the thermal optimization of a miniature heat pipe with a grooved wick structure [J]. *Journal of Heat Mass Transfer*, 2003, 46: 2051–2063.
- [6] SUMAN B, KUMAR P. An analytical model for fluid flow and heat transfer in a micro-heat pipe of polygonal shape [J]. *International Journal of Heat and Mass Transfer*, 2005, 48: 4498–4509.
- [7] KANG S W, TSAI SH H, CHEN H C H. Fabrication and test of

- radial grooved micro heat pipes [J]. Applied Thermal Engineering, 2002, 22: 1559–1568.
- [8] GILLOT C, AVENAS Y, CEZAC N, POUPON G. Silicon heat pipes used as thermal spreaders [J]. IEEE Transactions on Components and Packaging Technologies, 2003, 2: 332–339.
- [9] LEE M, WONG M, ZOHAR Y. Integrated microheat pipe fabrication technology [J]. Journal of Micro Electromechanical Systems, 2003, 2: 138–146.
- [10] CHEN S W, HSIEH J C. Experimental investigation and visualization on capillary and boiling limits of micro-grooves made by different processes [J]. Sensors and Actuators A, 2007, 139: 78–87.
- [11] LI Yong, XIAO Hui. Forming method of axial micro grooves inside copper heat pipe [J]. Transactions of Nonferrous Metals Society of China, 2008, 18: 1229–1212.
- [12] NAKAYAMA W, DAIKOKU T, KUWAHARA H. Dynamic model of enhanced boiling heat transfer on porous surfaces (part I): Experimental investigation [J]. J Heat Transfer Trans ASME, 1980, 102: 445–450.
- [13] LIU Xiao-qing, TANG Yong, PAN Ming-qiang, JIANG Le-lun. Manufacturing heat pipe by combined ploughing-extrusion process [C]//Proceeding of the International Conference in Integration and Commercialization of Mico- and Nano-systems. Sanya, China: ASME, 2007: 1417–1422.
- [14] CHEN Pin, TANG Yong, LIU Xiao-kang, LIU Xiao-qing. Formation of integral fins function-surface by extrusion-ploughing process [J]. Transaction of Nonferrous Metals Society of China, 2006, 16: 1029–1034.
- [15] CHI Yong, TANG Yong, CHEN Jin-chang, DENG Xue-xiong, LIU Lin, WAN Zhen-ping, LIU Xiao-qing. Forming process of cross-connected finned microgrooves in copper strips [J]. Transactions of Nonferrous Metals Society of China, 2007, 17: 267–272.

## 热柱吸液芯的成形方法

陶素连<sup>1,2</sup>, 汤勇<sup>1</sup>, 潘敏强<sup>1</sup>, 万珍平<sup>1</sup>, 陆龙生<sup>1</sup>

1. 华南理工大学 表面功能结构先进制造广东普通高校重点实验室, 广州 510640;
2. 广东水利电力职业技术学院 机械工程系, 广州 510635

**摘要:** 设计了热柱蒸发端和冷凝端吸液芯的结构, 采用犁切-挤压加工方法成形热柱吸液芯, 分析热柱吸液芯犁切-挤压成形特征、条件及成形机理。分析表明: 犁切-挤压深度对吸液芯表面形貌起决定作用, 犁切-挤压深度越大, 表面形貌越好; 沟槽间距只有在一定的范围内, 才能形成优异的表面形貌。实验结果表明: 当犁切-挤压深度为 0.3 mm、环状沟槽间距为 0.4 mm、径向沟槽夹角为 3°时, 热柱蒸发端形成较优的强化沸腾结构; 当犁切-挤压深度为 0.3 mm、环状沟槽间距为 0.4 mm、轴向沟槽间距为  $\pi/3$  mm 时, 热柱冷凝端形成较优的冷凝强化结构。

**关键词:** 热柱; 吸液芯; 犁切-挤压; 传热; 沟槽

(Edited by YANG Hua)